The hydrologic cycle in deep-time climate problems

Raymond T. Pierrehumbert

Department of the Geophysical Sciences, The University of Chicago, 5734 South Ellis Avenue, Chicago, Illinois 60637, USA (e-mail: rtp1@geosci.uchicago.edu)

Hydrology refers to the whole panoply of effects the water molecule has on climate and on the land surface during its journey there and back again between ocean and atmosphere. On its way, it is cycled through vapour, cloud water, snow, sea ice and glacier ice, as well as acting as a catalyst for silicate–carbonate weathering reactions governing atmospheric carbon dioxide. Because carbon dioxide affects the hydrologic cycle through temperature, climate is a *pas des deux* between carbon dioxide and water, with important guest appearances by surface ice cover.

When sunlight evaporates water from the ocean surface, the energy is stored in the form of latent heat in atmospheric water vapour. The flow of this fluid sunshine to distant places, where it releases its energy by condensation, forms one of the main modes of energy transport in the atmosphere. Water also affects the radiation balance of the planet through the water vapour greenhouse effect and cloud greenhouse effect, and through reflection of sunlight by clouds and ice. The rate of precipitation of water from the atmosphere determines the rate of chemical weathering of silicate rocks, and hence ultimately the carbon dioxide content of the atmosphere. In the following review, I will discuss in turn the way these three aspects of the hydrologic cycle helped to make past climates of the Earth so different from the present one.

The 'snowball Earth' concept provides stimulus for thinking about the hydrologic cycle in climates radically different from the present. Snowball Earth refers to a situation in which the ocean becomes ice-covered all the way from the poles to the tropics, possibly with the accompaniment of near-total land coverage by glaciers. There is evidence that this happened at least twice during the Neoproterozoic, about 600–700 million years ago[1,2].

In discussing water and energy transport, I focus principally on differences in pole-to-equator temperature gradients in warm and cold climates. An interplay of latent heat scaling, temperature gradient and eddy activity conspires to keep net north–south atmospheric energy transport relatively unchanged between Last Glacial Maximum (LGM) conditions and Cretaceous-style hothouse conditions, although the constancy is expected to break down both in ultra-cold snowball conditions and in ultra-warm conditions prevailing in the aftermath of deglaciating a snowball.

My discussion of the radiative effects of water vapour focuses on cloud, water vapour and ice-albedo feedbacks as they affect the conditions for initiation and termination of the snowball state (for a broader review of radiative water vapour feedbacks, see refs 3, 4). The principal conclusion here is that most questions one might wish to address regarding snowball Earth are exquisitely and distressingly sensitive to the details of cloud behaviour.

Finally, in discussing the weathering effects of water, I emphasize the way energetic considerations constrain the precipitation–temperature relation. Low precipitation (and hence slow weathering) is unambiguously and unsurprisingly expected in cold conditions, but in sufficiently warm conditions energetic limits come into play that significantly affect the operation of the silicate weathering thermostat.

Water vapour and energy transport

The answer to virtually every grand-challenge climate problem hinges on the behaviour of the pole-to-equator temperature gradient ΔT, or equivalently, the meridional heat transport carried by the atmosphere and ocean. The latent heat content of water vapour can have a profound effect on the efficiency with which heat is transported.

ΔT affects the initiation of ice ages, with high ΔT making it easier to grow glaciers and sea ice at high latitudes. But in very cold, low-CO_2 climates, a low ΔT makes it easier for ice to penetrate into the tropics and trigger a global glaciation. The threshold CO_2 needed to deglaciate a snowball state depends critically on ΔT, as a large value makes it easier to melt tropical ice, wherafter ice-albedo feedback takes care of the rest of the planet. A small value of ΔT helps to explain the Cretaceous and similar climates, as it is then possible to keep the poles ice-free with moderate elevations of greenhouse gas concentrations, without violating observational constraints on tropical temperatures.

It has long been noted that warm climates like that of the Cretaceous tend to have smaller ΔT than the present, whereas cold climates like that of the LGM have much larger ΔT, a phenomenon known as 'polar amplification'. Polar amplification is also apparent in projections of global warming, in that doubled-CO_2 experiments show greater warming at the poles than in the tropics. This overall picture of climate change has been damaged by recent revisions to estimates of LGM and Cretaceous tropical temperature, but not destroyed. On the cold side, LGM Greenland temperatures[5], together with recent estimates of tropical cooling[6], suggest that the surface temperature difference between 75 °N and the tropics increased to 50 K from its modern annual-mean value of about 33 K. On the warm side, deep-sea Eocene and Early Palaeocene temperatures[7] suggest polar temperatures of 283–287 K, with similar (or even warmer) values prevailing in the Cretaceous[8]. Recently, it has been argued that the tropics warmed much more during the Cretaceous than previously believed, potentially up to 4 K warmer than the present tropics[9]. Even the hot-tropics scenario yields a ΔT of 19–23 K, which is considerably lower

than the present value, although not so much so as the more conventional cool-tropics scenario. Can changes in latent heat flux account for polar amplification?

The meridional fluxes of dry and moist energy are:

$$F_d(\phi) = <\rho c_p v T + \rho g v Z>,\ F_w(\phi) = <\rho v L q> \quad (1)$$

where F_d and F_w are the fluxes of dry static energy and latent heat, ϕ is latitude, ρ is air density (including water vapour), c_p is the mean specific heat of air (again including water vapour), v is meridional velocity, Z is geopotential height, L is latent heat of condensation and q is the specific humidity (that is, the proportion of water vapour to the total mass of the air). The dry static energy is dominated by vT in the mid-latitudes, but the geopotential term becomes important in the tropics. Angle brackets denote an integral over altitude and an average along the latitude circle. Figure 1 shows an estimate of the annual-mean dry and moist fluxes for the years 1979 to 1995, recomputed from the data described in ref. 10. In the tropics, the latent heat flux is actually towards the Equator, owing to the transport of moist air in the low-level branch of the Hadley circulation. The equatorward latent heat transport is more than cancelled by the poleward flux of dry static energy. Net tropical flux is made poleward by the vZ term, characterizing the warming of air due to compression in the sinking branch of the circulation. Moisture actually makes it harder for the Hadley cell to transport heat out of the deep tropics, because the same circulation that warms the subtropics by compressional heating and cools the deep tropics by adiabatic expansion of rising air, of necessity also carries latent heat from the subtropics into the deep tropics. In the mid-latitudes, the latent heat flux is poleward, attaining a maximum value of about 2 petawatts (PW, or 10^{15} W), which is approximately half of the total flux.

How might this situation change in a much warmer or much colder climate? In the mid-latitudes, the net flux can be estimated by

$$F_d + F_w \sim <\rho> V c_p \left(\delta T + \frac{L \delta q}{c_p} \right) \quad (2)$$

where V is the typical meridional velocity scale, δT is the typical temperature fluctuation (assumed to be proportional to ΔT) and δq is the typical specific humidity fluctuation. Moisture is picked up at the subtropical ocean surface, which is nearly saturated. Because the heat-transporting atmospheric trajectories go poleward and upward, the relevant moisture contrast that the mixing acts upon is not between the high- and low-latitude values of boundary-layer specific humidity, but rather between the low-latitude values and the values aloft, which are essentially zero by virtue of the low temperatures there. Thus, I estimate δq as $q_s(T)$, where T is the subtropical temperature and q_s is the saturation specific humidity. Now, one can define the equivalent temperature $T^* = L\delta q_s / c_p$, which is the size of temperature fluctuation that would yield a dry heat transport equivalent to that due to moisture.

A graph of T^* is given in Fig. 2. At high temperature, the atmosphere is all steam, $q_s \rightarrow 1$ and $T^* \rightarrow 1{,}250$ K. In this limit, transport is wholly dominated by moisture. Moreover, a very weak wind suffices to produce an enormous heat flux. At temperatures of around 290K, the scaling correctly predicts dry and moist heat fluxes to be equally important. As the slope is large at these temperatures, the importance of moisture changes greatly even for modest changes in T, on the order of 4 K. Latent heat transport is still an important factor for temperatures near freezing, but T^* falls to 1 K at 250 K, at which point latent heat transports are essentially negligible. Completing the estimate of heat transport requires a theory of how V changes as ΔT and moisture change. This unfortunately is beyond the state of the art, and so I confine further discussion to an examination of latent heat flux changes in a range of climate simulations.

The LGM provides an excellent laboratory for studying the behaviour of heat fluxes in a colder climate. In view of the considerable increase in ΔT at the LGM, one might expect greatly elevated heat

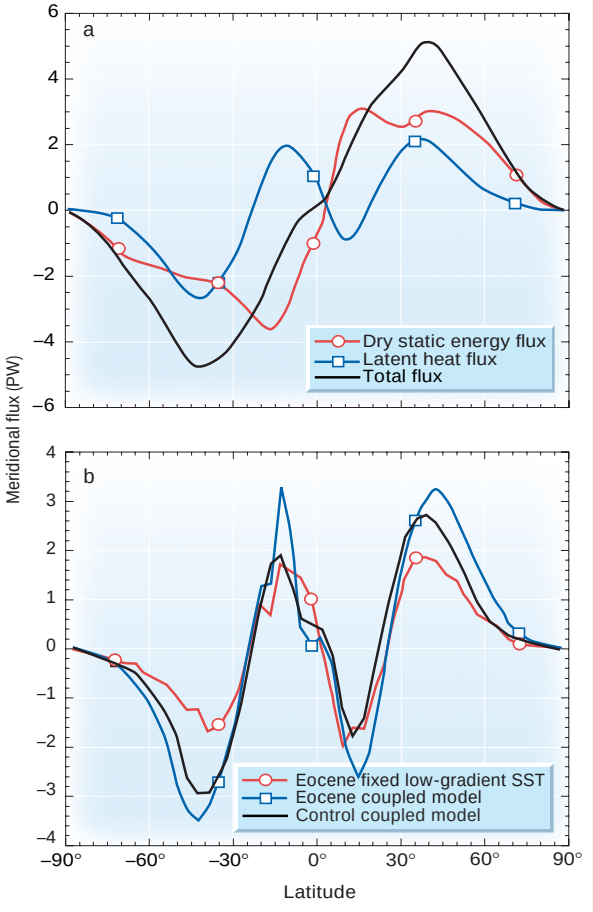

Figure 1 Northward heat flux in the atmosphere, broken down into moist and dry contributions. **a**, Observed annual-mean atmospheric energy transports computed from analyses made by the National Centers for Environmental Prediction. **b**, Latent heat flux from simulations of pre-industrial modern climate (control coupled model) and two hypothetical Eocene climates (simulations carried out with fixed low-gradient SST or with a coupled atmosphere–ocean model). Heat flux expressed in petawatts (1 PW = 10^{15} W).

fluxes. Increasing ΔT makes δT bigger in equation (2) and also makes V bigger, as an increased gradient provides a greater energy supply for synoptic eddies. In fact, simulations show little increase in the heat exported from the tropics by atmospheric fluxes[11,12]. This is largely because a drop in latent heat transport associated with cooler subtropics compensates the increase in dry static energy transport, but there are also subtle dynamical issues involved[13]. An important consequence of the relative constancy of the heat export is that introduction of Northern Hemisphere ice sheets alone does little to cool the tropics; one must instead invoke CO_2 reductions and oceanic effects — perhaps amplified by cloud and water vapour feedbacks — to get the deep tropics to cool much. Energy-balance models that simply diffuse temperature will seriously misrepresent fluxes in such climates. Incorporating a hydrologic cycle by diffusing moisture horizontally fails to take into account the importance of lifting and cooling of air parcels. However, more sophisticated idealized models incorporating more dynamical processes[14] show considerable promise.

The hard-snowball state provides an example of a yet colder climate. For a frozen Earth, there is little thermal inertia so the temperature pattern responds instantaneously to the seasonal cycle of insolation. In winter, polar temperatures fall to 190 K and the tropics are a chilly 240 K (see ref. 15; the mixed-layer simulation discussed in

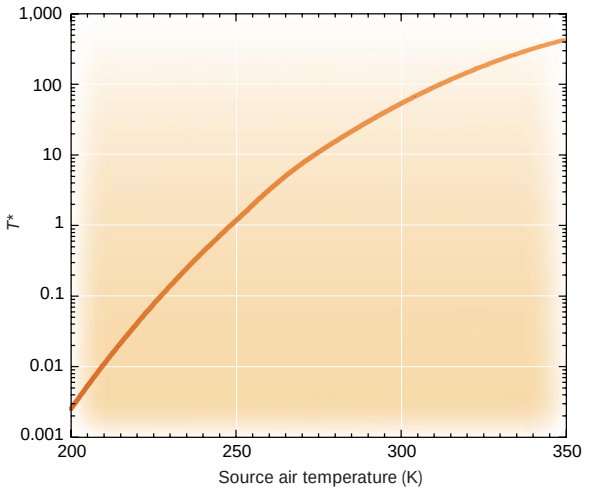

Figure 2 Characteristic temperature determining the relative importance of latent heat flux as a function of surface temperature. $T^*(T)$ is the magnitude of temperature fluctuation needed for dry heat transport to equal latent heat transport by water vapour. The graph shows the increasing dominance of latent heat flux as temperature increases.

ref. 16 yields similar values). In such a cold climate, there would be little or no latent heat flux, which is probably why such a large gradient can be maintained despite the fact that the weak solar absorption by ice means that little heat needs to be transported to even out the gradient. As CO_2 increases and the tropics warm towards freezing point, latent heat should become significant. It is an open question, though, whether the temperature gradient decreases as deglaciation is approached.

Atmospheric heat fluxes cannot maintain the low ΔT believed to have prevailed in the Cretaceous, and it has been conjectured that ocean heat transports could supply the missing flux[17]. But recent simulations from coupled atmosphere–ocean models do not support this supposition. In a model generated by the Geophysical Fluid Dynamics Laboratory in Princeton, permanent polar ice can be eliminated with a CO_2 level of 1,200 p.p.m., but under these conditions the tropics also warm considerably, reaching zonal mean temperatures of 302 K, or about 5 K warmer than the present tropics[18].

Transport statistics are not available for this model run, so instead I present computations based on a series of Eocene simulations carried out with a climate system model developed by the National Center for Atmospheric Research (see refs 19, 20 for a description of the simulations). Latent heat fluxes for the Eocene are shown in Fig. 1b. The simulation labelled 'Eocene fixed' was carried out with fixed low-gradient sea surface temperature (SST) with $\Delta T = 17$ K and tropical temperatures of 300 K, conditions that suppress polar ice. Case 'Eocene coupled' was carried out with a coupled atmosphere–ocean model with Eocene geography and an elevated CO_2 level of 560 p.p.m. For comparison, a modern pre-industrial simulation with CO_2 at 280 p.p.m. is included (case 'Control coupled'); the flux for this case is similar to that yielded in higher-resolution simulations driven by observed modern SST (not shown). The Eocene coupled simulation leads to warming in both the tropics and the polar regions as compared to the control, but not enough to eliminate polar ice completely. The warming is 2 K in the tropics, but 7 K at latitudes 50 °N and 50 °S where ice has been melted. There is thus a modest reduction in temperature gradient out to these latitudes.

In the Eocene-fixed simulation, the lower gradient reduces V and the greater moisture content of subtropical and mid-latitude air is not able to compensate; as a consequence, the flux drops considerably in comparison to present-day fluxes. In the Eocene-coupled case, the ocean fluxes are not sufficient to maintain a low gradient, so the tropical temperature warms considerably. Although this increase does lead to a modest increase of 0.5 PW over the control in peak mid-latitude latent heat flux, it is insufficient to substantially affect the gradient.

Going into cold climates, the attenuation of the hydrologic cycle has the expected effect of reducing latent heat fluxes and allowing a larger pole-to-equator temperature gradient than would otherwise be possible. Going into warm climates, the increase in moisture content is offset by a reduction in eddy activity, and thus the heat transport changes little. Enhanced polar warming occurs in those regions where ice has disappeared, but the temperature gradient is not further moderated by latent heat feedbacks. The behaviour of latent heat flux makes it harder rather than easier to maintain a low-gradient Cretaceous or Eocene world. Current observational developments[9] are contributing towards a better understanding of how low a gradient really needs to be explained, although this intriguing development must be regarded as tentative until it is confirmed by more (and preferably farther offshore) data. Future refinements of ocean dynamics or of radiative mechanisms[21] offer some hope for reduction of the gradients in coupled simulations. The chasm has not yet been bridged, but it no longer seems quite so wide as it once did.

Radiative effects of water

The chief questions regarding snowball Earth are: How could Earth enter the snowball state and, once there, how could it get out? The latter is particularly important to the viability of the snowball hypothesis, as it is indisputable that if the Earth indeed were ever in a snowball state, it eventually deglaciated. Scenarios for entering the snowball state invariably posit attainment of anomalously low CO_2 concentrations, helped along by the 6% fainter Sun prevailing in the Neoproterozoic. Exit strategies conversely call on greatly elevated CO_2 concentrations; estimates based on thickness of cap carbonates or the likely amount of CO_2 degassed during the glaciated period would be consistent with deglaciation at CO_2 partial pressures in the vicinity of 0.2 bar. At present, it is impossible to rule out the possibility of much higher CO_2 concentrations at deglaciation, but the weak logarithmic dependence of the outgoing long-wave radiation (OLR) on CO_2 means that doubling or tripling the estimate of maximum allowable CO_2 at deglaciation does not greatly alter the picture presented here. The radiative properties of water vapour and clouds enter crucially in both the glaciation and deglaciation problems.

There have been several studies of initiation of the snowball state using general circulation models (GCMs) coupled to a mixed-layer ocean without ocean dynamics[15,22,23]. Some succeed in triggering a global glaciation when CO_2 is reduced to 100 p.p.m., and others do not, with no clear picture emerging on the controlling factors. The use of specified ocean heat transports estimated from the present ocean in such models is problematic. Certainly, if ocean heat transports are eliminated altogether, the Earth falls easily into a snowball state at low CO_2, although dynamic ocean heat transport has been found to be a potent inhibitor of glaciation[16]. The coupled-model results in ref. 16 should not, however, be construed as ruling out the possibility of global glaciation, in view of the relatively short simulations used, the highly idealized sea-ice model, and myriad other uncertainties plaguing ocean simulation.

There has been less study of the deglaciation problem. Deglaciation studies have been limited to idealized energy balance models[24], as current GCMs do not generally take into account all absorption bands that become important at high CO_2, and often assume that CO_2 is a trace gas for the purpose of convective and thermodynamic computation. But the sensitivity of global glaciation and deglaciation to water vapour and clouds may present a severe impediment to obtaining conclusive results from either theoretical or modelling studies.

I will use an idealized model to quantify the importance of cloud and water vapour effects. The temperature of a solar-heated planet is determined by the amount of energy received from the Sun and the

temperature required to allow the planet to lose the required amount of energy to space. In the simplest form of climate model, I characterize the entire planet by a single surface temperature T, which one may think of as the global-mean temperature. The temperature is then determined by solving

$$(1-\alpha(T))L/4 = I_{+}(T, \mathrm{pCO_2}, \mathrm{RH}, \mathrm{clouds}) \quad (3)$$

where α is the planetary albedo (dependent on T via temperature dependence of cloud and ice cover), L is the solar constant at the planet's orbit, and I_{+} is the outgoing infrared radiation flux exiting the top of the atmosphere. For a given temperature, I_{+} depends on the concentration $\mathrm{pCO_2}$, the atmospheric relative humidity RH, and an array of cloud parameters. For clear skies, I computed $I_{+}(T, \mathrm{pCO_2}, \mathrm{RH})$ using a radiation model[25], which can accurately handle arbitrarily high CO_2. The vertical profile of temperature is assumed to be the moist adiabat proceeding from the specified surface temperature T, patched to an isothermal stratosphere. Relative humidity is assumed constant in height, at a stipulated value. The assumption of fixed relative humidity implies that the water vapour content of each layer of the atmosphere increases with temperature in proportion to the local water-holding capacity, expressed by the Clausius–Clapeyron

Box 1

Climate sensitivity and the dependence of outgoing long-wave radiation on temperature

A planet can lose energy to outer space only through emission of electromagnetic radiation. For the range of planetary temperatures typically considered, this radiation is in the infrared range, and the flux of the outgoing radiation is known as outgoing long-wave radiation (OLR). The temperature of a solar-heated planet settles at the value that allows the OLR to balance the absorbed solar radiation; hence the shape of the dependence of OLR on temperature holds the key to the most fundamental climate phenomena. For an atmosphere-free planet having a uniform surface temperature T, the OLR would satisfy the Stefan–Boltzman law, σT^4. Atmospheres modify the OLR by allowing the planet to radiate at temperatures colder than the planetary surface. The consequent decrease in OLR is a direct consequence of the fact that temperature decreases with height, and thus the strength of the greenhouse effect is sensitive to the lapse rate.

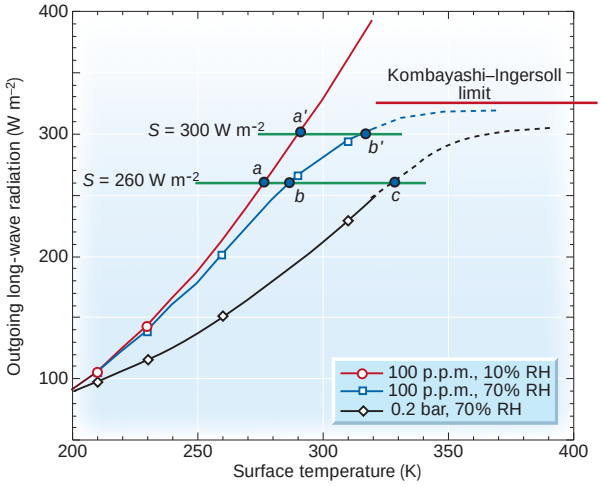

The figure opposite shows OLR as a function of surface temperature, computed under the following assumptions: (1) the vertical temperature profile is given by the moist adiabat, patched to a 200-K isothermal stratosphere, and (2) the specific humidity at each height is a fixed fraction of the saturation value given by the temperature at that height. The latter assumption is known as the 'fixed relative-humidity assumption'. Once these assumptions are made, the OLR can be computed as a function of the surface temperature using any standard radiative-transfer model (the curves here were computed using the model of ref. 25).

Addition of a greenhouse gas to an atmosphere reduces the OLR for fixed T, with the result that temperature must increase in order to bring the radiation budget back into balance. For absorbed solar radiation $S = 260$ W m^{-2}, 100 p.p.m. CO_2 and 10% relative humidity, the temperature is 276 K (point *a* in the figure). If the relative humidity is increased to 70%, the temperature increases to 288 K (point *b*). If the greenhouse forcing is further augmented by massively increasing the amount of CO_2 to 0.2 bar, the temperature increases to ~330 K (point *c*).

Because the concentration of water vapour (a greenhouse gas) increases with temperature, it acts to reduce the slope of the OLR curve. This increases the sensitivity of climate to changes in radiative forcing, as is illustrated in the figure by increasing solar absorption to 300 W m^{-2}. With 10% relative humidity, the warming from point *a* to *a′* is 14 K, but with 70% relative humidity, the warming from point *b* to *b′* is 30 K. This is known as the water vapour feedback. The ultimate water vapour feedback is the runaway greenhouse, manifest in the fact that the flattening of the OLR curve at high temperatures leads it to asymptote to a value known as the Kombayashi–Ingersoll limit. This is the limit to how fast a planet with a moist atmosphere can loose energy by infrared radiation. For a saturated atmosphere, the limit depends primarily on the gravity of the planet, which determines the mass of atmosphere contained above a given pressure level. The precise value one obtains for the limit depends on the treatment of infrared absorption properties of water vapour at high temperature and pressure. In the figure above, we have sketched in the value from ref. 42 (about 320 W m^{-2}), and the reader is referred there for further details.

When the solar forcing exceeds the Kombayashi–Ingersoll limit, the temperature continues to increase until the surface temperature is several thousand degrees, at which point all the ocean has been evaporated into the atmosphere. This is followed by disassociation of water into hydrogen and oxygen, after which the light hydrogen escapes to space making the water loss irreversible. Once there is no precipitating water reaching the ground, it becomes impossible to bind up atmospheric carbon dioxide in carbonate rocks. This scenario, or some version of it, is the prevailing view of how Venus was consigned to a climate so much less habitable than Earth's. The Kombayashi–Ingersoll limit is also relevant to impact heating of planets during their early stages, as it determines how quickly a planet can condense out the transient post-impact steam atmosphere.

The assumption of fixed relative humidity is a convenient starting point for simple models, but as the atmosphere aloft is highly undersaturated, it is dubious to consider humidity to be strictly a function of local temperature. Atmospheric humidity is in reality governed by a bewildering array of dynamical and microphysical processes for which useful idealized models are not yet available. Clouds pose an even greater challenge. The picture of the runaway greenhouse given above was based on clear-sky reasoning, but a saturated atmosphere would be thick with clouds. These clouds would block nearly all solar radiation, but would also be very effective at limiting OLR. The resulting climate would be determined by the delicate balance between a trickle of incoming solar radiation and a trickle of OLR, much as has been proposed to result from CO_2 clouds on early Mars. There have been a few tentative steps towards including clouds in the runaway greenhouse calculation[42], but the cloud physics regime in which the cloud-forming substance is the primary component of the atmosphere is a very unfamiliar one, and offers many exciting prospects for future work.

relation. This is far from inevitable, as air aloft is highly undersaturated. However, the fixed relative humidity *ansatz* does seem to capture the radiative behaviour of water vapour in full GCMs[3]. Most climate phenomena, including water vapour feedback, can be understood in terms of the shape of $I_+(T)$, also known as OLR (see Box 1).

Following common practice, the surface albedo $\alpha_s(T)$ is fixed at the value α_i for ice for temperatures $T<T_i$ where the planet is completely frozen, and at the smaller ice-free value α_o for $T>T_o$ when the planet is assumed ice-free. For $T_i<T<T_o$ one linearly interpolates between the limiting values. The presumed pole-to-equator temperature difference enters into the choice of T_i and T_o, as both temperatures would be equal to the freezing point of water for an isothermal planet, but the two values separate as ΔT increases. The cloudy-sky planetary albedo is then determined as a function of α_s and the cloud albedo α_c, using equation (1) in ref. 26. The albedos do not simply add, because sunlight reflected by the clouds does not have the opportunity to be further reflected by the surface. Thus, clouds over ice have a weaker effect on absorbed solar radiation than do clouds over ocean. In contrast, clouds have nearly the same effect on reducing OLR regardless of the underlying surface. As a result, the net cloud effect is a weak cooling over low-albedo surfaces, but adds up to a significant warming over ice. Because of this asymmetry, clouds profoundly affect initiation and termination thresholds.

Cloud albedo was parameterized as a function of T by assuming cloud water path to be a fixed fraction (10%) of saturation humidity at each height, and then calculating the top-of-atmosphere albedo using a radiative-transfer model[27]. In this parameterization, the cloud albedo vanishes at very low temperatures where there is little water in the air; however, the albedo remains significant even near the freezing point, as it takes rather little water to make a radiatively significant cloud. To determine cloudy-sky OLR, I assumed a fixed mean cloud-top temperature, and assumed that the cloud tops are high enough to control the OLR without reference to the greenhouse gases in the overlying atmosphere. This is equivalent to fixing the cloudy-sky OLR at a stipulated value OLR_{cloud}. I have tested this assumption against calculations with a full radiation model in which cloud water content is assumed proportional to saturation humidity, and found it to be accurate. From the standpoint of OLR, clouds act much like water vapour except that, kilogram for kilogram, their infrared activity is much more potent. Increasing the atmospheric temperature increases the mass of cloud water, causing the atmosphere to radiate from higher altitudes, with the result that the effective radiating temperature changes little with surface temperature — much as in the runaway greenhouse (Box 1). In this cloud parameterization, water vapour itself has no effect on OLR.

For both OLR and albedo, the radiation balance is completed by blending the clear-sky and cloudy values according to a specified cloud fraction. Additionally, the albedo is adjusted so as to allow for solar absorption by the atmosphere. Of course, clouds are not just a function of temperature. They are strongly affected by microphysics and dynamics, among other things. For example, there are few high clouds in the subsiding subtropical regions, despite the warm temperatures there. In the idealized model, all such effects are wrapped into the effective cloud fraction, which will be varied as a free parameter. Feedbacks arising from systematic changes in cloud fraction as the climate state changes cannot be treated in this formulation, but one can still gain an appreciation of the kind of climate that accompanies a given amount of cloudiness.

Unless CO_2 concentration is extremely high, a fully glaciated Earth reflects enough sunlight to remain frozen until CO_2 increases enough to trigger deglaciation. This is true even for present conditions. The problem is not maintaining the snowball state, but rather accounting for how the system can be forced into that state from a state with ice cover (if any) limited to high latitudes. Thus I consider the system to initiate a snowball only when the stable ice-free or partially ice-covered state ceases to exist, in which case the planet is forced to enter a snowball state regardless of the initial conditions.

Figure 3 shows regime diagrams indicating where, as a function of cloud fraction and clear-sky relative humidity, the snowball state initiates at 100 p.p.m. CO_2, and where the state deglaciates when CO_2 is raised to 0.2 bar. These choices are somewhat arbitrary, but serve as a reasonable basis for probing the sensitivity of the system. When $OLR_{cloud} = 120$ W m^{-2}, the snowball state is initiated when there is sufficient cloud cover, with less cloud cover needed at low relative humidity (note that, in these calculations, relative humidity refers to the humidity of the clear-sky areas between clouds). However, there is no combination of cloud cover and humidity that allows the planet to deglaciate. When $OLR_{cloud} = 90$ W m^{-2}, the clouds have greater warming effect and the planet can deglaciate. Under these conditions, however, the planet does not enter the snowball state unless humidity and cloud cover are severely reduced. When $OLR_{cloud} = 100$ W m^{-2}, there is a tiny sliver of parameter space in which the planet can both initiate and deglaciate a snowball, but initiation requires dry, clear-sky conditions. Note that there is considerable sensitivity to clear-sky humidity even (in fact, especially) under dry conditions. Small amounts of water vapour can make a big difference to climate, because the radiative effect of water vapour is logarithmic in the water vapour concentration[3,4].

The results are consistent with GCM studies which show that (at least in the absence of dynamic ocean heat fluxes) it is possible to initiate a snowball state even in the face of cloud feedbacks, and that cloud feedback can actually help the initiation. But it is particularly unsettling that changes in the cloud radiative properties by less than 30 W m^{-2} can completely change the regime outcome; this number is well within the uncertainty of cloud parameterizations even for the well-observed modern climate. It comes as no surprise, then, that GCMs should differ so much in their initiation behaviour. To be fair, it must be said that clouds are not the only, or even chief, source of uncertainty. Small changes in the ice albedo, for example, can also have significant consequences; indeed, the difficulty in achieving globally glaciated states in the simulations of Chandler and Sohl[23] may have been due at least in part to the use of an unrealistically low

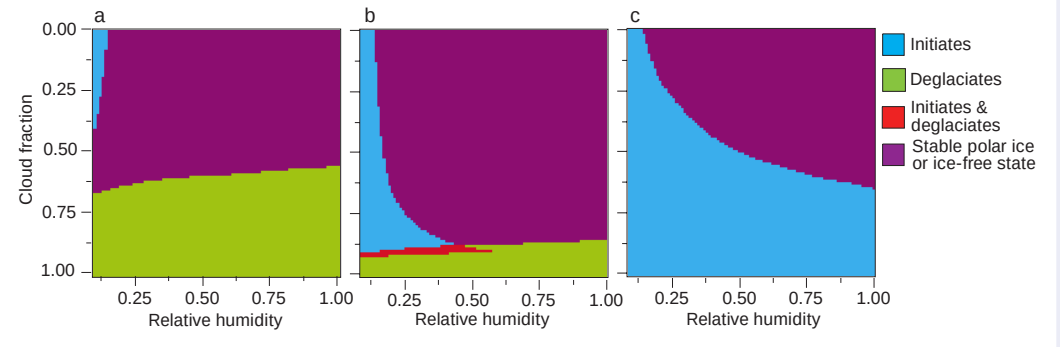

Figure 3 Regime diagrams showing effects of cloud cover and clear-sky relative humidity on initiation and termination of the snowball Earth state. All calculations were carried out with Neoproterozoic insolation, and an ice albedo of 0.7. **a**, $OLR_{cloud} = 90$ W m^{-2}; **b**, $OLR_{cloud} = 100$ W m^{-2}; **c**, $OLR_{cloud} = 120$ W m^{-2}.

ice albedo. There is no one single, true value for ice albedo, and the range of surface types that need to be considered offers interesting and novel possibilities for additional radiative feedbacks[28].

Another implication of these results is that termination of the snowball state cannot occur at plausible CO_2 levels without considerable help from cloud effects. It is encouraging to see that there are at least plausible settings of fundamental optical cloud properties that allow the snowball state to terminate, as previous estimates of the termination threshold fixed the net cloud radiative forcing at its present value[24] — clearly a perilous assumption in view of the disparate influence of clouds over ice compared with clouds over water.

The snowball Earth problem has the paradoxical implication that it is now necessary to understand very warm climates — much warmer than the Cretaceous — which are nonetheless short of the conditions for a runaway greenhouse. Such climates occur in the aftermath of the snowball state, when the planet has deglaciated but CO_2 levels are still at the high levels attained during the frozen state. Based on the idealized model with 50% cloud cover and 50% relative humidity, and $OLR_{cloud} = 100\ W\ m^{-2}$, the mean temperature rises to 332 K in the aftermath; at 100% relative humidity it would be 345 K. Happily the deglaciation does not trigger a runaway greenhouse, which would be catastrophic for both life on Earth and the viability of the snowball hypothesis. The tropical temperatures that accompany these mean temperatures depend on the efficiency of horizontal heat transport. From Fig. 2, it is clear that transports would be dominated by latent heat, but the temperature gradient nonetheless remains an open question, because it is unknown how the intensity of heat-transporting eddies would scale in such a warm climate.

A further challenge to modelling the post-snowball climate is that water vapour makes up over 10% of the total air pressure, so that precipitation has a marked effect on surface pressure, and hence dynamics. The consequences of this feedback are not invariably incorporated in current circulation models, and represent very unfamiliar territory, but some pioneering work in this direction can be found in ref. 29.

Precipitation–temperature relation and weathering

Four billion years ago, the Sun was about 30% fainter than it is at present, and yet the Earth did not spend its first three billion years of life in an unrelenting snowball state. This is known as the 'faint young Sun' problem[30]. The currently favoured resolution is that CO_2 concentration was much higher earlier in the Earth's history, and that feedback between temperature and weathering of silicate rocks into carbonate controlled CO_2 levels so as to maintain an equable climate (ref. 31; and see refs 32, 33 for a discussion of the earlier literature as well as current thinking on the subject).

In the prevailing view, temperature affects chemical weathering primarily through its effect on precipitation. It is thus the presumed increase of precipitation with temperature that leads to the stabilizing CO_2 thermostat. Although GCMs do yield increased precipitation in response to modest increases in temperature, it is not generally recognized that there are energetic constraints limiting the slope of the precipitation–temperature relation. If the temperature difference δT_s between the boundary-layer air and the surface is not too large, the surface energy budget can be linearized to yield

$$S_{surf} = E + F = (E_o(T) + a(T)\delta T_s) + (F_o + b(T)\delta T_s) \quad (4)$$

where S_{surf} is the surface-absorbed solar radiation, E is the evaporative heat flux, F is the sum of radiative and sensible heat fluxes. The flux coefficients are given by

$$E_o = \rho L k_{turb}(1-r)q_s(T), \qquad a = L k_{turb} r \frac{d\rho q_s}{dT},$$
$$F_o = \sigma g(T) T^4, \qquad b = 4\sigma T^3 + \rho k_{turb} c_p \quad (5)$$

where k_{turb} is the turbulent exchange coefficient, σ is the Stefan–Boltzmann constant, and r is the boundary-layer relative humidity. Much dynamics is hidden in the determination of r, which in the following will be simply taken as a specified parameter. $g(T)$ is a coefficient describing the net infrared radiative cooling of the surface, taking into account the back radiation from the atmosphere into the surface. Above 310 K, g is essentially zero regardless of CO_2, owing to dominance of water vapour. By solving equation (4) for δT_s one finds the following expression for the evaporation, which in steady state must equal the precipitation

$$E(T) = E_o + (S - E_o - F_o)\frac{a}{a+b} \quad (6)$$

At cold temperatures, both terms become exponentially small owing to the paucity of water in the atmosphere. As temperature increases, E_o increases exponentially and F_o vanishes, but the coefficient $a/(a+b)$ becomes close to unity, limiting the growth of

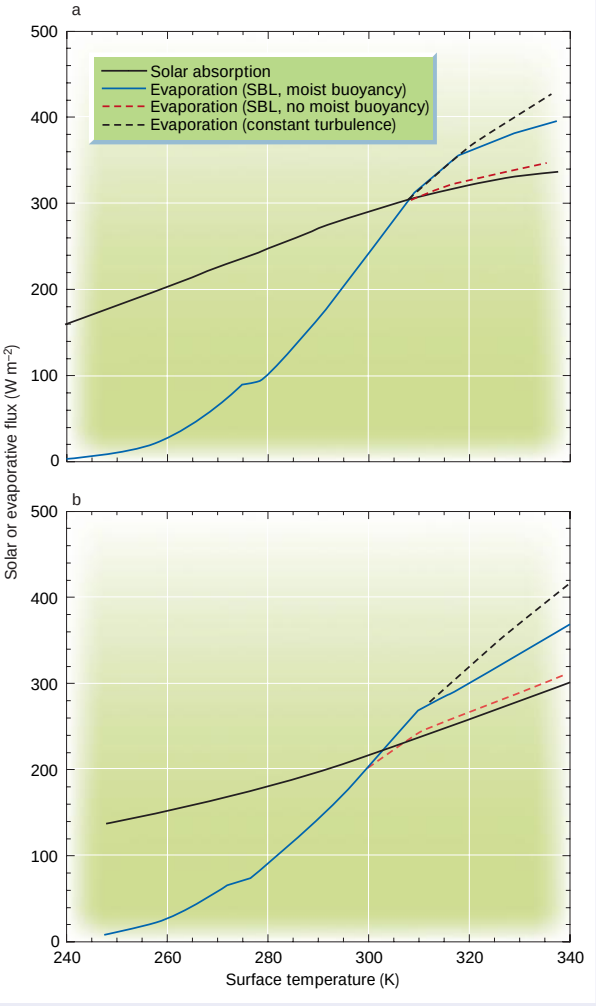

Figure 4 Relation between precipitation and temperature. The mean evaporation from the surface is shown as a function of the surface temperature, together with the amount of solar radiation needed to maintain that temperature. **a**, Low-CO_2 case (100 p.p.m. CO_2 in atmosphere); **b**, high-CO_2 case (0.2 bar). In a steady state, precipitation is equal to evaporation, and 1 W m^{-2} of evaporation from a liquid surface corresponds to 1.26 cm yr^{-1} of liquid-equivalent precipitation (1.11 cm yr^{-1} for the case of sublimation from an ice surface). The estimates are based on a radiative–convective model, as described in the text. Evaporation is computed for three alternate boundary-layer assumptions: fixed turbulence, stable boundary-layer physics (SBL) including buoyancy effects of water vapour, and stable boundary-layer physics neglecting buoyancy effects of water vapour.

evaporation. However, the exponential increase of E_o allows evaporation to exceed the available solar radiation in very warm conditions. This is possible in energetic terms because the surface becomes colder than the atmosphere, so that the missing energy can be supplied by sensible heat flux from the atmosphere into the surface. The use of a constant k_{turb} is implausible in this case, as turbulent transfer through the stable boundary layer would be greatly inhibited[34]. Furthermore, convection would be choked off, limiting the import of dry air that keeps $r<1$ and sustains evaporation.

It is common practice in climate models to suppress boundary-layer turbulence when the boundary layer becomes stably stratified[35]. In determining the stability of the boundary layer, there is another factor that needs to be taken into account — water vapour is lighter than dry air. Moisture 'dissolving' in dry air can cause it to rise just as salt dissolving in the surface of a tank of fresh water can cause water to sink. This effect becomes particularly significant at warm temperatures, when water vapour makes up a considerable fraction of the mass of saturated air. The buoyancy of water vapour is represented conventionally by virtual temperature, which is the temperature a dry-air parcel would need to have in order to yield the same density (at fixed pressure) as the moisture-laden parcel[36]. Virtual temperature always exceeds the actual temperature, allowing the boundary layer to be unstable even if the surface is somewhat colder than the overlying drier air. For example, if the boundary-layer relative humidity is 80% while the surface layer is saturated, then surface air at 320 K is positively buoyant when $\delta T_s > -1.44$ K.

In the results presented below, an idealized boundary-layer parameterization is used, which gradually shuts off the turbulent transfer when the virtual temperature of the saturated air in contact with the surface becomes colder than that of the overlying air. For comparison, results neglecting the effect of water vapour on buoyancy, and results with constant k_{turb}, are also shown. Calculations were carried out with a maximum k_{turb} of 0.016 m s^{-1} (corresponding to a wind speed of 8 m s^{-1} in neutrally stratified conditions), and with boundary-layer relative humidity $r = 0.8$.

To complete the problem, the top-of-atmosphere energy budget must also be satisfied. This is accomplished using a radiative–convective model similar to that of the previous section, except that a small (and largely inconsequential) allowance for the effect of δT on OLR is included, and the atmospheric solar absorption is neglected so as to make interpretation of the results more straightforward. Results for a low-CO_2 (100 p.p.m.) and a high-CO_2 (0.2 bar) case are shown in Fig. 4. Because we are interested specifically in understanding the precipitation–temperature relation, the surface temperature is taken as the independent variable and plots show the solar forcing S needed to maintain the stated temperature, along with the associated evaporation. As solar forcing balances OLR in a steady state, the curves of S versus temperature are nothing more than OLR curves of the sort shown in Box 1.

An interesting point is that the solar absorption affects precipitation even for fixed temperature. This is because evaporation cools the surface, and if there is not enough solar energy to offset the cooling, the surface cools sufficiently to limit further evaporation. Consider two planets, each with a surface temperature of 300 K. The first has high CO_2 concentration, and the surface temperature is sustained by a faint sun yielding 218 W m^{-2} of absorbed solar radiation (Fig. 4b). The precipitation in this case is 258 cm yr^{-1}. The second planet has low CO_2 concentration and needs a brighter sun to sustain it, with absorbed solar radiation 291 W m^{-2} (Fig. 4a). This planet is bathed by 307 cm yr^{-1} of precipitation. Neither of these estimates is dependent on stable boundary-layer physics, as the evaporation is not great enough to drive δT_s negative. The planet with the fainter sun has weaker weathering, and so would have to warm to a higher temperature for the weathering to balance the same amount of CO_2 outgassing as would be in equilibrium in the bright-sun planet. This could be part of the reason that snowball states were not ubiquitous early in Earth's history. When the Sun is faint, the whole hydrologic cycle is sluggish, and so with less weathering it is harder to draw CO_2 down to levels sufficiently low to initiate the snowball state.

A distinct change in regime occurs when the evaporation exceeds the absorbed solar radiation (Fig. 4), by which point the surface has become colder than the overlying air. Past this point (about 302 K in the high-CO_2 case), precipitation increases more slowly with temperature. Without the destabilizing effects of water vapour buoyancy, evaporation is limited to a value only slightly in excess of the absorbed solar radiation. In this case the silicate–carbonate weathering thermostat breaks down, as increases in temperature fail to increase precipitation (for a fixed solar brightness) and so cannot halt accumulation of CO_2 in the atmosphere. Incorporating the virtual temperature effect helps sustain boundary-layer turbulence and allows precipitation to exceed solar radiation by a greater margin. But the effectiveness of the thermostat is compromised. For example, for a planet in equilibrium with 300 W m^{-2} of solar absorption, increasing CO_2 from 100 p.p.m. to 0.2 bar increases temperature from 307 K to 340 K, but evaporation is increased by only 66 W m^{-2}, yielding only a 22% increase in weathering rate. Neglecting boundary-layer stabilization altogether and keeping turbulence fixed would allow a somewhat greater increase.

A definitive treatment of precipitation in very warm climates would require a much more sophisticated boundary-layer calculation than that presented here. The point of the calculation I have discussed is that the continued operation of the weathering thermostat in very warm climates depends intimately on what is going on in the boundary layer, and on the myriad processes that affect the surface energy budget. These considerations are crucial to the rate of recovery of CO_2 in very warm climates in the aftermath of a snowball Earth deglaciation. Calibration of the precipitation–temperature relation with GCM experiments using fixed surface temperature will yield incorrect results in warm climates, as such calculations do not respect the surface energy budget.

At cold temperatures, in contrast, the surface energy budget is not a significant constraint, and precipitation decreases exponentially in accordance with the decreasing amount of water vapour available in the atmosphere. The reduction of weathering in cold climates is unambiguous, and the weathering thermostat should work well to inhibit runaway glaciation. Initiation of a snowball state proceeds from a temporary breakdown of the thermostat on the cold side. It has been conjectured that anomalous weathering rates could result from a preponderance of tropical continents[1], or from methane-induced precipitation enhancement (D. P. Schrag , R. A. Berner, P. F. Hoffman & G. P. Halverson, personal communication, 2002).

Once a hard snowball is achieved, the tropical temperatures drop to 250 K or less, at which point precipitation rates of only a few centimetres per year are indicated (Fig. 4; GCMs that achieve a hard snowball often yield even less precipitation). Glacial dynamics is driven by a balance between ice flow and precipitation, so it is far from clear that much glacial erosion could be supported by such a small precipitation rate, which is comparable to that found in the very interior of Antarctica today. Geological evidence is unambiguous in indicating active glacial erosion in conjunction with snowball events[37,38], but it is possible (although not certain) that the active glaciers are confined to the beginning and end of the glaciated period[2]. At the end of the glaciated period, when enough CO_2 has accumulated to warm the tropics to around 270 K, the precipitation rises to 50 cm yr^{-1} (Fig. 4), and active glaciers are not problematic. Active glaciers at the beginning of the snowball period could arise at times before the tropics is completely frozen.

Weak though it is, the remanent hydrologic cycle during the hard snowball has potentially important consequences for the erosion of ice cover. Because ice thickness is determined ultimately by a small geothermal heat flux, weak evaporation can have a major impact on ice thickness (see ref. 39, although more recent work with improved models of solar absorption in ice indicates substantial modifications to the exploratory results reported there[28]). Just as a small amount of

evaporation can thin ice, small amounts of precipitation can thicken it, and perhaps more important, increase its albedo. The full implications of the sluggish-snowball hydrologic cycle are only beginning to be explored.

Other planets, other hydrologies

Hydrologic systems analogous to Earth's water-based hydrology can be built upon other condensable greenhouse gases, any of which have multiple roles as greenhouse gas, cloud-forming substance and latent heat transporter. Examples include methane on Titan[40] and CO_2 on early Mars[41]. A unique feature of the CO_2–water system is the interaction between the hydrologic cycle of one greenhouse gas (water) and the weathering chemistry determining the concentration of the other greenhouse gas (CO_2). One wonders whether these are the only substances on which a thermostatic feedback loop can be built, or if other planets in the Universe may have found alternate solutions to the problem of maintaining habitability. □

doi:10.1038/nature01088

1. Hoffman, P. F., Kaufman. A. J., Halverson, G. P. & Schrag, D. P. A Neoproterozoic snowball earth. *Science* **281,** 1342–1346 (1998).
2. Hoffman, P. F. & Schrag, D. P. The snowball Earth hypothesis: testing the limits of global change. *Terra Nova* (in the press).
3. Held, I. M. & Soden, B. J. Water vapor feedback and global warming. *Annu. Rev. Energ. Environ.* **25,** 441–475 (2000).
4. Pierrehumbert, R. T. in *Mechanisms of Global Change at Millennial Time Scales* (eds Clark, P. U., Webb, R. S. & Keigwin, L. D.) Geophys. Monogr. Ser. 112 (American Geophysical Union, Washington DC, 1999).
5. Dahl-Jehnsen, D. *et al.* Past temperatures directly from the Greenland Ice Sheet. *Science* **282,** 268–271 (1998).
6. Lea, D. W., Pak, D. K. & Spero, H. J. Climate impact of late quaternary Pacific equatorial sea surface temperature variations. *Science* **289,** 1719–1724 (2000).
7. Lear, C. H., Elderfield, H. & Wilson, P. A. Cenozoic deep-sea temperatures and global ice volumes from Mg/Ca in benthic foraminiferal calcite. *Science* **287,** 269–272 (2000).
8. Huber, B. T. Tropical paradise at the Cretaceous poles? *Science* **282,** 2199–2200 (1998)
9. Pearson, P. N. *et al.* Warm tropical sea surface temperatures in the Late Cretaceous and Eocene epochs. *Nature* **413,** 481–487 (2001).
10. Trenberth, K. E. & Caron, J. M. Estimates of meridional atmosphere and ocean heat transports. *J. Clim.* **14,** 3433–3443 (2001).
11. Manabe, S. & Broccoli, A. J. The influence of continental ice sheets on the climate of an ice age. *J. Geophys. Res.* **90(C2),** 2167–2190 (1985).
12. Broccoli, A. J. Tropical cooling at the last glacial maximum: an atmosphere-mixed layer ocean model simulation. *J. Clim.* **13,** 951–976 (2000).
13. Hall, N. M. J., Dong, B. & Valdes, P. J. Atmospheric equilibrium, instability and energy transport at the last glacial maximum. *Clim. Dynam.* **12,** 497–511 (1996).
14. Sokolov, A. P. & Stone, P. H. A flexible climate model for use in integrated assessments. *Clim. Dynam.* **14,** 291–303 (1998).
15. Jenkins, G. S. & Smith, S. R. GCM simulations of Snowball Earth conditions during the late Proterozoic. *Geophys. Res. Lett.* **26,** 2263–2266 (1999).
16. Poulsen, C., Pierrehumbert, R. T. & Jacob, R. Impact of ocean dynamics on the simulation of the Neoproterozoic "Snowball Earth". *Geophys. Res. Lett.* **28,** 1575–1578 (2001).
17. Barron, E. J., Fawcett, P. J., Peterson, W. H., Pollard, D. & Thompson, S. L. A simulation of mid-Cretaceous climate. *Paleoceanography* **10,** 953–962 (1995).
18. Bush, A. B. & Philander, S. G. H. The late Cretaceous: simulation with a coupled atmosphere-ocean general circulation model. *Paleoceanography* **12,** 495–516 (1997).
19. Huber, M. & Sloan, L. C. Heat transport, deep waters, and thermal gradients: coupled simulation of an Eocene Greenhouse Climate. *Geophys. Res. Lett.* **28,** 3481–3484 (2001).
20. Huber, M. & Sloan, L. C. Climatic responses to tropical sea surface temperature changes on a "greenhouse" Earth. *Paleoceanography* **15,** 443–450 (2000).
21. Kirk-Davidoff, D. B., Schrag, D. P. & Anderson, J. G. On the feedback of stratospheric clouds on polar climate. *Geophys. Res. Lett.* (in press).
22. Hyde, W. T.., Crowley, T. J., Baum, S. K. & Peltier, W. R. Neoproterozoic 'snowball Earth' simulations with a coupled climate-ice sheet model. *Nature* **405,** 425–429 (2000).
23. Chandler, M. A. & Sohl, L. E. Climate forcings and the initiation of low-latitude ice sheets during the Neoproterozoic Varanger glacial interval. *J. Geophys. Res.* **105,** 20737–20756 (2000).
24. Caldeira, K. & Kasting, J. F. Susceptibility of the early Earth to irreversible glaciation caused by carbon-dioxide clouds. *Nature* **359,** 226–228 (1992).
25. Kasting, J. F., Pollack, J. B. & Ackerman, T. P. Response of Earth's atmosphere to increases in solar flux and implications for loss of water from Venus. *Icarus* **57,** 335–355 (1984).
26. Pierrehumbert, R. T. & Erlick, C. On the scattering greenhouse effect of CO_2 ice clouds. *J. Atmos. Sci.* **55,** 1897–1903 (1998).
27. Briegleb, B. P. Delta-Eddington approximation for solar radiation in the NCAR Community Climate Model. *J. Geophys. Res.* **97,** 7603–7612 (1992).
28. Warren, S. G., Brandt, R. E., Grenfell, T. C. & McKay, C. P. Snowball Earth: ice thickness on the tropical ocean. *J. Geophys. Res.* (in the press).
29. Hay, W. W., DeConto, R. M. & Wold, C. N. Climate: is the past the key to the future? *Geol. Rundsch.* **86(2),** 471–491 (1997).
30. Sagan, C. & Mullen, G. Earth and Mars—evolution of atmospheres and surface temperatures. *Science* **177,** 52–56 (1972).
31. Walker, J. C. G., Hays, P. B. & Kasting, J. F. A negative feedback mechanism for the long-term stabilization of Earth's surface-temperature. *J. Geophys. Res.* **86(Nc10),** 9776–9782 (1981).
32. Berner, R. A. GEOCARB II: a revised model of atmospheric CO_2 over Phanerozoic time. *Am. J. Sci.* **294,** 56–91 (1994).
33. Berner, R. A. & Kothavala, Z. GEOCARB III: a revised model of atmospheric CO_2 over phanerozoic time. *Am. J. Sci.* **301,** 182–204 (2001).
34. Vogelezang, D. H. P. & Holtslag, A. A. M. Evaluation and model impacts of alternative boundary-layer height formulations. *Bound. Layer Meteorol.* **81,** 245–269 (1996).
35. Kiehl, J. T. *et al.* The National Center for Atmospheric Research Community Climate Model: CCM3. *J. Climate* **11,** 1131–1149 (1998).
36. Emanuel, K. A. *Atmospheric Convection* (Oxford Univ. Press, New York, 1994).
37. Christie-Blick, N., Sohl, L. E. & Kennedy, M. J. Considering a Neoproterozoic snowball Earth. *Science* **284,** 1087 (1999).
38. McMechan, M. E. Vreeland diamictites-Neoproterozoic glaciogenic slope deposits, Rocky Mountains, northeast British Columbia. *Can. Bull. Petrol. Geol.* **48,** 246–261 (2000).
39. McKay, C. P. Thickness of tropical ice and photosynthesis on a snowball Earth. *Geophys. Res. Lett.* **27,** 2153–2156 (2000).
40. Lunine, J. I., Lorenz, R. D. & Hartmann, W. K. Some speculations on Titan's past, present and future. *Planet Space Sci.* **46,** 1099–1107 (1998).
41. Forget, F. & Pierrehumbert, R. T. Warming early Mars with carbon dioxide clouds that scatter infrared radiation. *Science* **278,** 1273–1276 (1997).
42. Kasting, J. F. Runaway and moist greenhouse atmospheres and the evolution of Earth and Venus. *Icarus* **74,** 472–494 (1988).

Acknowledgements

I am indebted to K. Trenberth, M. Huber and C. Poulsen for providing data used in this review, and for much other valuable assistance. P. Hoffman and D. Schrag introduced me to the snowball Earth problem, and our discussions on this subject have continued over the years; insofar as I understand anything at all about the phenomenon, much credit is due to them. I also benefited from comments by R. Alley, T. Schneider and S. Warren. I had the further advantage of meetings and discussions carried out as part of my participation in the NOAA Panel on Abrupt Climate Change, for which the support of the National Oceanographic and Atmospheric Administration is gratefully acknowledged.